Clinical Cancer Research

Targeting Notch Signaling with a Notch2/Notch3 Antagonist (Tarextumab) Inhibits Tumor Growth and Decreases Tumor-Initiating Cell Frequency

Wan-Ching Yen, Marcus M. Fischer, Fumiko Axelrod, Christopher Bond, Jennifer Cain, Belinda Cancilla, William R. Henner, Rene Meisner, Aaron Sato, Jalpa Shah, Tracy Tang, Breanna Wallace, Min Wang, Chun Zhang, Ann M. Kapoun, John Lewicki, Austin Gurney, and Timothy Hoey

Abstract

Purpose: The Notch pathway plays an important role in both stem cell biology and cancer. Dysregulation of Notch signaling has been reported in several human tumor types. In this report, we describe the development of an antibody, OMP-59R5 (tarextumab), which blocks both Notch2 and Notch3 signaling.

Experimental Design: We utilized patient-derived xenograft tumors to evaluate antitumor effect of OMP-59R5. Immunohistochemistry, RNA microarray, real-time PCR, and *in vivo* serial transplantation assays were employed to investigate the mechanisms of action and pharmacodynamic readouts.

Results: We found that anti-Notch2/3, either as a single agent or in combination with chemotherapeutic agents was efficacious in a broad spectrum of epithelial tumors, including breast, lung, ovarian, and pancreatic cancers. Notably, the sensitivity of anti-Notch2/3 in combination with gemcitabine in pancreatic tumors was associated with higher levels of *Notch3* gene expression. The antitumor effect of anti-Notch2/3 in combination with gemcitabine plus *nab*-paclitaxel was greater than the combination effect with gemcitabine alone. OMP-59R5 inhibits both human and mouse Notch2 and Notch3 function and its antitumor activity was characterized by a dual mechanism of action in both tumor and stromal/vascular cells in xenograft experiments. In tumor cells, anti-Notch2/3 inhibited expression of Notch target genes and reduced tumor-initiating cell frequency. In the tumor stroma, OMP-59R5 consistently inhibited the expression of *Notch3*, *HeyL*, and *Rgs5*, characteristic of affecting pericyte function in tumor vasculature.

Conclusions: These findings indicate that blockade of Notch2/3 signaling with this cross-reactive antagonist antibody may be an effective strategy for treatment of a variety of tumor types. *Clin Cancer Res; 21(9); 2084–95. ©2015 AACR.*

Introduction

The Notch pathway is one of several key pathways linked to both stem cell biology and cancer (1). In particular, dysregulated Notch2 and/or Notch3 activity has been associated with several human tumor types, including lung (2), ovarian (3), breast (4), pancreatic (5, 6), and colon cancers (7). In addition to its role in developmental biology and cancer, Notch signaling also plays a key role in tumor vasculature and pericytes (8). Thus, therapeutic strategies directed at inhibition of the Notch2/3 pathway on tumors and vasculature may offer promise for the treatment of solid tumors.

Accumulating evidence has indicated that tumors are frequently composed of heterogeneous cell types that vary in their ability to initiate new tumor growth and that cancer stem cells (CSC, also referred to as tumor-initiating cells) drive tumor growth and progression and are relatively resistant to many existing therapies, including conventional chemotherapy and radiation treatments (9, 10). Because aberrant Notch signaling has been implicated in cancer, cancer stem cells, and tumor vasculature, therapeutic strategies that effectively target Notch signaling could have a major impact on cancer patient survival. Although inhibition of Notch receptor cleavage enzymes by gamma-secretase inhibitors (GSI) have been developed and progressed in the clinic, the therapeutic utility of these compounds is limited due to intestinal toxicity resulting from pan-Notch inhibition (11). In the current study, we report the development of a novel cross-reactive antibody OMP-59R5 that selectively inhibits the function of both Notch2 and Notch3. We evaluated antitumor effect of anti-Notch2/3 antibody and its mechanisms of actions using patient-derived xenograft (PDX) models.

Materials and Methods

Antibody generation and characterization

OMP-59R5 was generated by panning the HuCAL GOLD phage-display library (MorphoSys AG; ref. 12) with recombinant Notch2 extracellular domain (EGF1–12) containing the ligand-binding site. DNA fragments encoding the fAb generated from the phage display library were subcloned into a full-length human IgG2 expression vector and subsequently expressed into CHO cells and purified. To determine the ability of OMP-59R5 to block

OncoMed Pharmaceuticals, Inc., Redwood City, California.

Note: Supplementary data for this article are available at Clinical Cancer Research Online (http://clincancerres.aacrjournals.org/).

Current address for C. Bond: CDRD—The Centre for Drug Research and Development, Vancouver, British Columbia; current address for A. Sato: Sutro Biopharma, Inc., South San Francisco, California.

Corresponding Author: Wan-Ching Yen, OncoMed Pharmaceuticals Inc., 800 Chesapeake Drive, Redwood City, CA 94063. Phone: 650-995-8273; Fax: 650-298-8600; E-mail: jean.yen@oncomed.com

doi: 10.1158/1078-0432.CCR-14-2808

Translational Relevance

Aberrant Notch signaling has been implicated in cancer, cancer stem cells, and tumor vasculature. We report the development of OMP-59R5, an antibody that selectively inhibits the function of both Notch2 and Notch3. Our data demonstrate that OMP-59R5 was efficacious in inhibiting the growth of various epithelial tumors with minimal intestinal toxicity. Interference with Notch2/3 signaling by OMP-59R5 delayed tumor recurrence, decreased cancer stem cell frequency, and modulated the function of tumor vasculature. These findings provide evidence for the utility of targeting Notch2 and Notch3 for cancer treatment. Anti-Notch2/3 (tarextumab) is currently advancing in phase II clinical testing for treatment of pancreatic and small-cell lung cancers.

ligand binding to human Notch2 and Notch3 receptors, HEK 293 cells were transfected with cDNA expression vector encoding human Notch2 as well as a second vector encoding GFP, pcDNA-GFP, to mark the transiently transfected cells. Specific OMP-59R5 binding was assessed by determining the presence of cells positive for GFP signal and PE signal. For epitope mapping, HEK 293 cells were transiently transfected with expression vectors encoding human Notch2, human Notch1, or human Notch1 with residues 383–387 mutated to the corresponding human Notch2 residues. Cells were also cotransfected with a plasmid encoding GFP to mark those cells that received transfected plasmid. Cells were incubated with OMP-59R5 and fluorescent secondary antibody and then examined by FACS. The ability of antibodies to block activation of Notch signaling was determined by *in vitro* luciferase reporter assays as described previously (13). The binding affinities of OMP-59R5 were determined using a Biacore 2000. The data were fit using the simultaneous global fit equation to yield affinity constants (K_d) for each protein. Detailed assay protocols are described in Supplementary Materials and Methods.

In vivo animal studies

The establishment and characterization of minimally passed human tumor xenograft models were performed as previously described (13, 14). Sources of surgically removed patient tumors are CHTN (OMP-PN4, OMP-OV38), Asterand (OMP-LU40), and MRI (OMP-LU68). These tumors were established at OncoMed Pharmaceuticals, Inc. OMP-PN8, PN16, and PN17 and were obtained from Dr. Diane Simeone and UM-PE13 from Dr. Michael Clarke at the University of Michigan (Ann Arbor, MI). Cells were injected subcutaneously to NOD/SCID mice for efficacy studies. Treatment started when the mean tumor volumes reached about 100 mm^3. OMP-59R5 was dosed at 40 mg/kg every other week. Gemcitabine was given from 5 to 40 mg/kg in pancreatic tumor xenografts in Supplementary Table S3, except as indicated, that is, Fig. 4B and Fig. 4C. All chemotherapeutic agents were given once weekly. Both antibody and chemotherapeutic agents were administered intraperitoneally. The procedures for tumorigenicity study were described previously (14). CSC frequency was determined using L-Calc Version 1.1 software (StemCell Technologies). Differences in frequency between groups were analyzed by the likelihood-ratio test. Difference of $P < 0.05$ was considered significantly different. Detailed *in vivo* studies and *in vivo* limiting dilution assay (LDA) protocols are described in Supplementary Materials and Methods.

Real-Time RT-PCR, mRNA sequencing, and microarray gene expression

Tumor RNAs were isolated using the RNeasy Fibrous Tissue Mini Kit (Qiagen) with DNAseI treatment. Five-hundred nanograms total RNA was reverse transcribed into cDNA. Quantitative real-time PCR was performed in an ABI 7900 HT Fast Real Time PCR System and analyzed using the SDSv2.3 (Applied Biosystems). The results were normalized with the housekeeping gene *GADPH*. All primer and probe sets were obtained from Applied Biosystems. For microarray, samples were amplified using the Ovation RNA Amplification System V2 (NuGEN), adjusted for array background, normalized signal intensity with GCRMA algorithm in the open-source Bioconductor software (www.bioconductor.org), and profiled for mRNA expression using Affymetrix both HG-U133plus2 human and MG-430 2.0 mouse chips to assess treatment effects on human tumor cells and on mouse stroma cells independently. The probe sets that were not species-specific were omitted from the analysis. Data were subjected to the Gene Set Enrichment Analysis (GSEA). Genes differentially expressed between two groups were identified with the Bayesian *t* test (Cyber-T; ref. 15). Bayesian one-way ANOVA and Tukey HSD *post hoc* test were performed for experiments with more than two groups. The significantly regulated genes between groups or time points were chosen based on the *P* value <0.05 and absolute fold change $\geq$1.5. The sequencing libraries were prepared following the protocols supplied by Illumina for sequencing mRNA samples (Illumina CA). The FASTQ sequence reads were aligned to human genome hg19 and mouse genome mm9 with tophat (v2.0.9) and bowtie (v1.0.0). After the alignment of sequence reads, the uniquely mapped reads were counted for each gene by HTSeq python script (v0.5.3p9). The raw counts per gene in each xenograft tumor were then normalized as RPKM (reads per kilobase per million mapped reads) to represent the expression level of the gene in the tumor.

Histology

Whole tumors were excised and processed into formalin-fixed, paraffin-embedded (FFPE) slides or as nonfixed optimal cutting temperature (OCT, Tissue-Tek, Sakura) embedded slides. Immunohistochemistry slides were scanned using Imagescope (ScanScope AT, Aperio). Total nuclei, Ki67-labeled cells, staining area, and intensity were quantified by Aperio software after excluding necrotic regions. The primary antibody for immunohistochemistry (IHC) was anti-Ki-67 (Vector, VP-RM04) and for immunofluorescence were anti-CD31 (BD Biosciences, 550274) and anti-Desmin clone D93F5 (Cell Signaling Technology). Antipimonidazole (Hypoxyprobe) was used for intratumoral hypoxia detection. Detailed protocols for vascular perfusion, IHC, and immunofluorescence detections were described in Supplementary Materials and Methods.

Statistical analysis

Data for tumor measurements are expressed as mean $\pm$ SEM. Differences in mean values between groups were analyzed by the nonparametric *t* test. Multiple comparisons used a two-way ANOVA test followed by the Bonferroni post-test comparison. Differences of $P < 0.05$ are considered significantly different. Software for statistical analysis was by GraphPad Prism5 (GraphPad Software Inc.).

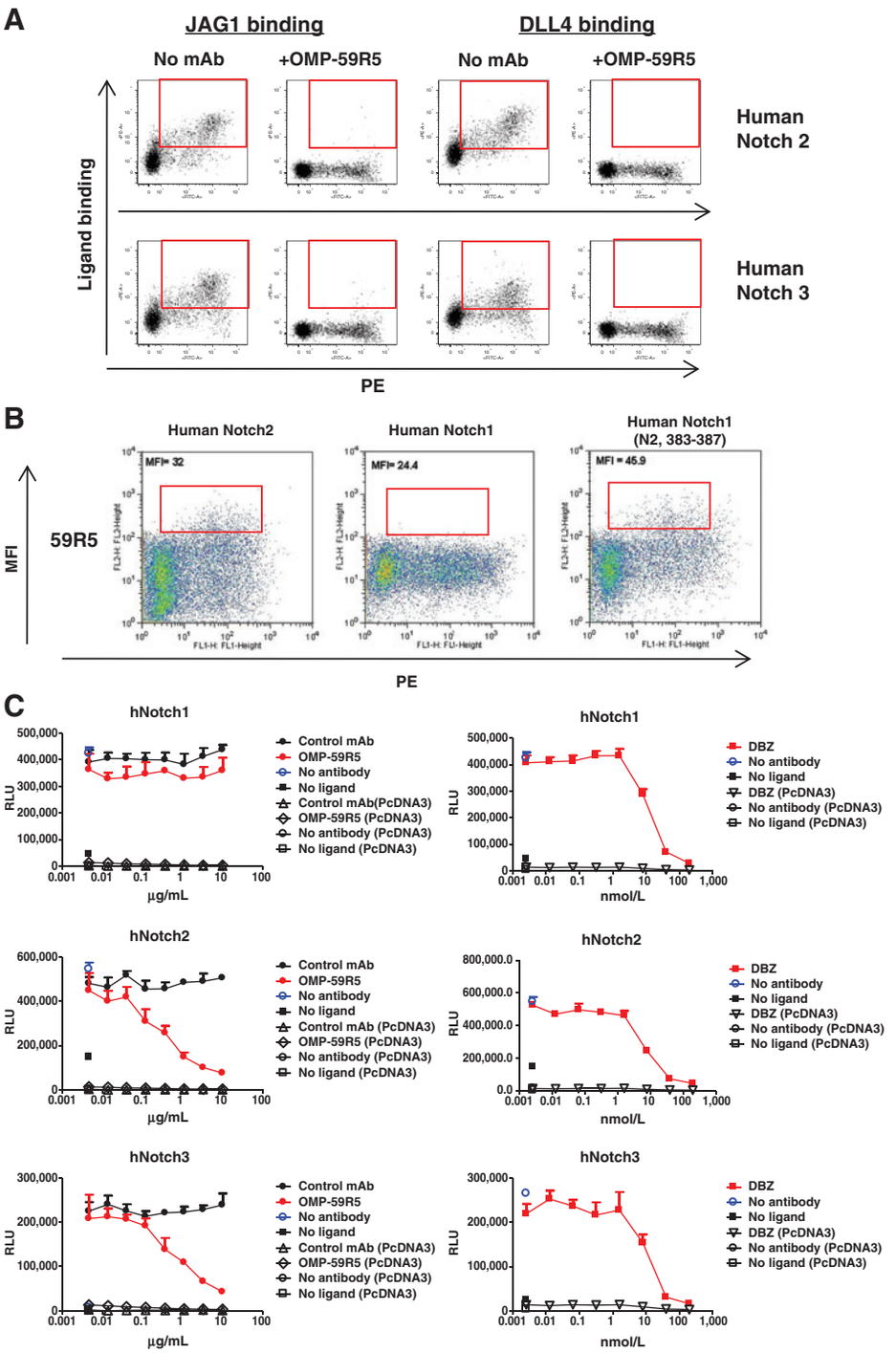

Figure 1.
Binding and blocking of OMP-59R5 to human and mouse Notch receptors. A, OMP-59R5 blocks ligand binding to Notch2 and Notch3. B, binding epitope of OMP-59R5 to human Notch2/3. C, effect of OMP-59R5 on blocking human Notch1, Notch2, and Notch3 signaling. Mean ± SD; $n = 3$ replicates. Right, gamma-secretase inhibitor DBZ-positive control. RLU, relative light units and is a unit of luciferase reporter activity.

Results

OMP-59R5 is a cross-reactive Notch2 and Notch3 antagonist

OMP-59R5 was identified using phase display (12) and was initially selected against human Notch2. Surface plasmon resonance-binding studies determined that this antibody demonstrates high-affinity binding to Notch2 and Notch3, with minimal binding to Notch1 and no detectable binding to Notch4 (Supplementary Fig. S1A). OMP-59R5 blocks Notch ligand DLL4 and JAG1 binding to human Notch2 (Fig. 1A). Analysis of deletion mutations identified EGF10 of Notch2 extracellular domains as required for binding (Note: due to the variance in the number of EGF repeats between the individual Notch family members, the corresponding EGF repeat of EGF10 in Notch2 is EGF9 in Notch3). Mutagenesis analysis revealed that OMP-59R5 binds to full-length human Notch2 and Notch1 with residues 383–387

mutated to the corresponding human Notch2 residues, but not to full-length Notch1 by flow cytometry (Fig. 1B), indicating that this region comprises at least part of the binding epitope. Alignment of the EGF9/10 region of Notch2 and Notch3 from rodent, human, and cynomolgus monkey indicated that both Notch2 and Notch3 are identical within the EGF repeat that contains the binding epitope of OMP-59R5 in several species (Supplementary Fig. S1B). Surface plasmon resonance further demonstrated that OMP-59R5 bound with high affinity to both Notch2 and Notch3 from mouse, rat, and human (Supplementary Table S1). Using a Notch-responsive luciferase reporter assay in HeLa cells, we demonstrated that OMP-59R5 effectively inhibited human Notch2 and Notch3 reporter activity but had no activity in blocking Notch1 signaling. In contrast, the gamma secretase inhibitor DBZ, a pan-Notch inhibitor, inhibited signaling from Notch1, Notch2, and Notch3 (Supplementary Fig. 1C).

OMP-59R5 inhibits xenograft tumor growth through reducing tumor cell proliferation and promotes differentiation

The effect of OMP-59R5 on tumor growth was accessed using a panel of minimally *in vivo* passaged PDX models (14). Engraftment in mice and drug treatment in these models has been shown to correlate with clinical outcome and treatment response (16, 17). These tumor models retain much of the heterogeneity of the original tumors enabling the study of the characterization of CSCs through serial transplantation (13, 14). The histologic features of these tumors are summarized in Supplementary Table S2. All tumors express human Notch1, Notch2, and Notch3 mRNA (Supplementary Fig. S2). OMP-59R5 treatment resulted in additional antitumor activity in combination with gemcitabine relative to gemcitabine alone in 6 of 10 tumors tested (Supplementary Table S3). In the most sensitive tumors, OMP-PN8 and OMP-PN17, combination therapy resulted in tumor regression beginning 2 weeks after treatment in OMP-PN8 and 3 weeks after treatment in OMP-PN17 (Supplementary Fig. S3). Histologic analysis in OMP-PN8 at the conclusion of the study revealed that OMP-59R5 single-agent treatment did not alter tumor cell morphology (hematoxylin and eosin), total tumor cell density (measured by total nuclei/mm^2), or cell proliferation (shown by Ki-67 immunoreactivity). Gemcitabine treatment resulted in 60% decrease in tumor cell density and 43% decrease in cell proliferation. The combination of OMP-59R5 and gemcitabine led to an additional 62% increase in apoptotic cell death and 52% reduction in tumor cell density versus gemcitabine ($P < 0.05$ in both cases). In the moderately differentiated adenocarcinoma OMP-PN21, OMP-59R5 treatment alone reduced tumor cell proliferation by 40% and promoted differentiation by inducing mucin-producing cells, as indicated by a 2.5-fold increase in Alcian blue staining compared with untreated controls (Fig. 2A). Gemcitabine treatment alone decreased cell proliferation by about 30% versus control, but had no effect on differentiation. Importantly, the combination therapy resulted in an additional 15% decrease in proliferating cells versus gemcitabine and induced a greater than 3-fold increase in Alcian blue staining ($P < 0.05$ in both cases). No apparent impact of OMP-59R5 on the intestinal morphology or increased secretory goblet cells was found at the dose used in these studies (Supplementary Fig. S4A). We did, however, observe an effect of OMP-59R5 on rodent teeth with long-term repeated high doses of OMP-59R5, beginning approximately 6 weeks after initiation of treatment (Supplementary Fig. S4B).

Sensitivity to OMP-59R5 is correlated with Notch3 expression in pancreatic tumors

Notably, the antitumor efficacy of OMP-59R5 in combination with gemcitabine was significantly associated with expression of human *Notch3* gene in pancreatic cancer. Tumors that were more sensitive to the OMP-59R5 plus gemcitabine combination (responders) versus gemcitabine alone had higher levels of *Notch3* baseline expression compared with tumors that showed no combination effect (nonresponders; Fig. 2B). The mean gene expression levels were significantly different between the responders and the nonresponders (10.44 in responders vs. 1.973 in nonresponders, $P = 0.0047$). The responsiveness of these tumors to the combination therapy was not associated with either Kras mutation status, sensitivity to gemcitabine, or molecular subtypes of pancreatic ductal adenocarcinoma as described by Collisson and colleagues previously (18), that is, classical (tumors express high adhesion-associated and epithelial genes with best survival prognosis), exocrine-like (tumors with high tumor cell-derived digestive enzyme genes), and quasi-mesenchymal (tumors with high mesenchyme-associated genes; Supplementary Table S3). In contrast to *Notch3*, there was no difference in *Notch1* or *Notch2* expression between responders and nonresponders (Supplementary Fig. S2). Thus, *Notch3* expression could be a useful predictive biomarker associated with sensitivity of OMP-59R5 in pancreatic cancer.

Pharmacodynamic effects in xenograft tumors treated with OMP-59R5

To identify pathways and gene sets regulated by OMP-59R5 in tumor cells, we isolated tumor RNA from four OMP-59R5–responsive tumors (OMP-PN4, PN8, PN16, and PN17) at the end of studies and analyzed for human and mouse gene expressions by microarray. GSEA revealed that OMP-59R5 downregulated the Notch pathway, oncogene signatures, cell proliferation gene sets, and several stem cell–related gene sets (Supplementary Table S4). Tumors treated with gemcitabine upregulated epithelial-to-mesenchymal (EMT) gene sets and a subset of the stem cell gene sets, consistent with our previous results indicating that gemcitabine promotes the EMT phenotype in pancreatic cancer (19). Notably, OMP-59R5 combination therapy reversed the increase in gemcitabine-induced expression of EMT gene sets and downregulated genes associated with embryonic stem cells (ESC) (ref. 20; Supplementary Table S4). Analysis of anti-Notch2/3 treatment on tumor stroma and vascular cells in xenografts revealed that *Notch3*, Notch target genes *Hey2*, *HeyL*, and *Rgs5*, a gene shown to mark pericytes (21) were consistently downregulated by OMP-59R5 treatment in the tumor stroma in all four pancreatic xenografts (Supplementary Table S5).

To confirm gene expression changes identified by microarray, we performed qRT-PCR analysis in OMP-PN17, a tumor that expresses high *NOTCH3* and responded to the combination therapy (Fig. 3A). Gemcitabine alone had no effect on Notch receptors or Notch target gene expression in OMP-PN17 xenograft tumors, whereas OMP-59R5 alone and in combination with gemcitabine downregulated human *NOTCH2*, *NOTCH3*, and *HES1*. *Notch3*, *Hes1*, *Rgs5*, and *HeyL* in the tumor stroma were inhibited by OMP-59R5 and the combination with gemcitabine compared with control monoclonal antibody (mAb)-treated tumors. OMP-59R5 had no effect on human *NOTCH1*, *JAG1*, and *JAG2* and mouse *Notch1*, *2*, and *4* gene expression. Similar effects were found in OMP-PN25, a high *NOTCH3*-expressing

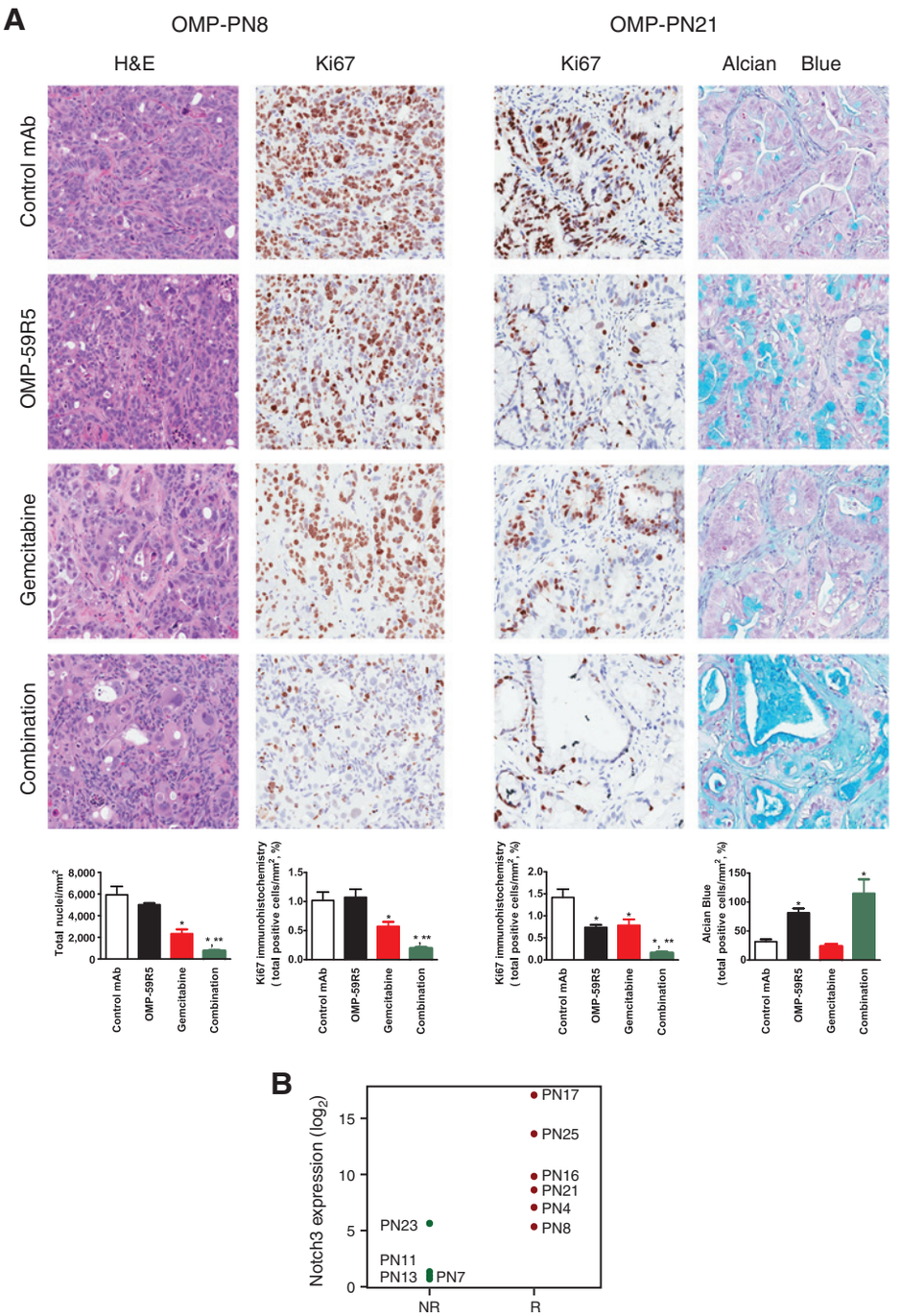

Figure 2.
In vivo efficacy of OMP-59R5 in pancreatic xenograft tumors. A, histologic evaluation of OMP-PN8 and OMP-PN21 xenograft tumors treated with OMP-59R5 and gemcitabine. Magnification, ×20. Quantification is expressed as mean ± SEM; $n = 3$–4 tumors per group. *, $P < 0.05$ vs. control mAb, **, $P < 0.05$ versus gemcitabine by the Bonferroni multiple comparison test. B, correlation of *NOTCH3* gene expression and efficacy of OMP-59R5 plus gemcitabine in pancreatic xenograft tumors. $P = 0.00047$ by the Welch *t* test in the mean gene expression levels between responders (R) and nonresponders (NR).

tumor and a combination therapy responsive xenograft that was not examined by microarray (Supplementary Fig. S5A). In addition, OMP-59R5 alone and the combination with gemcitabine downregulated *NANOG* and *OCT4*, two key genes that were found to be downregulated in ESC gene sets in tumor cells by GSEA. On the other hand, gemcitabine treatment had no effect or resulted in increased expression (Fig. 3A and Supplementary Fig. S5A). Real-time PCR analysis of EMT genes identified by GSEA in two of responsive tumors, OMP-PN8 and OMP-PN17, confirmed that gemcitabine induced mesenchymal gene expression (*CDH2*, *VIM*, *FN1*, *TWIST1*, *SNAI1*, *SNAI2*), whereas OMP-59R5 treatment and the combination therapy reversed or reduced these marker genes (Fig. 3A and Supplementary Fig. S5A). Immunohistochemical analysis further demonstrated that the combination therapy significantly decreased vimentin (VIM) expression in the tumor cells (Supplementary Fig. S5B). We also observed that, in OMP-PN17, OMP-59R5 treatment and the combination decreased protein levels of Notch3 receptor extracellular domain

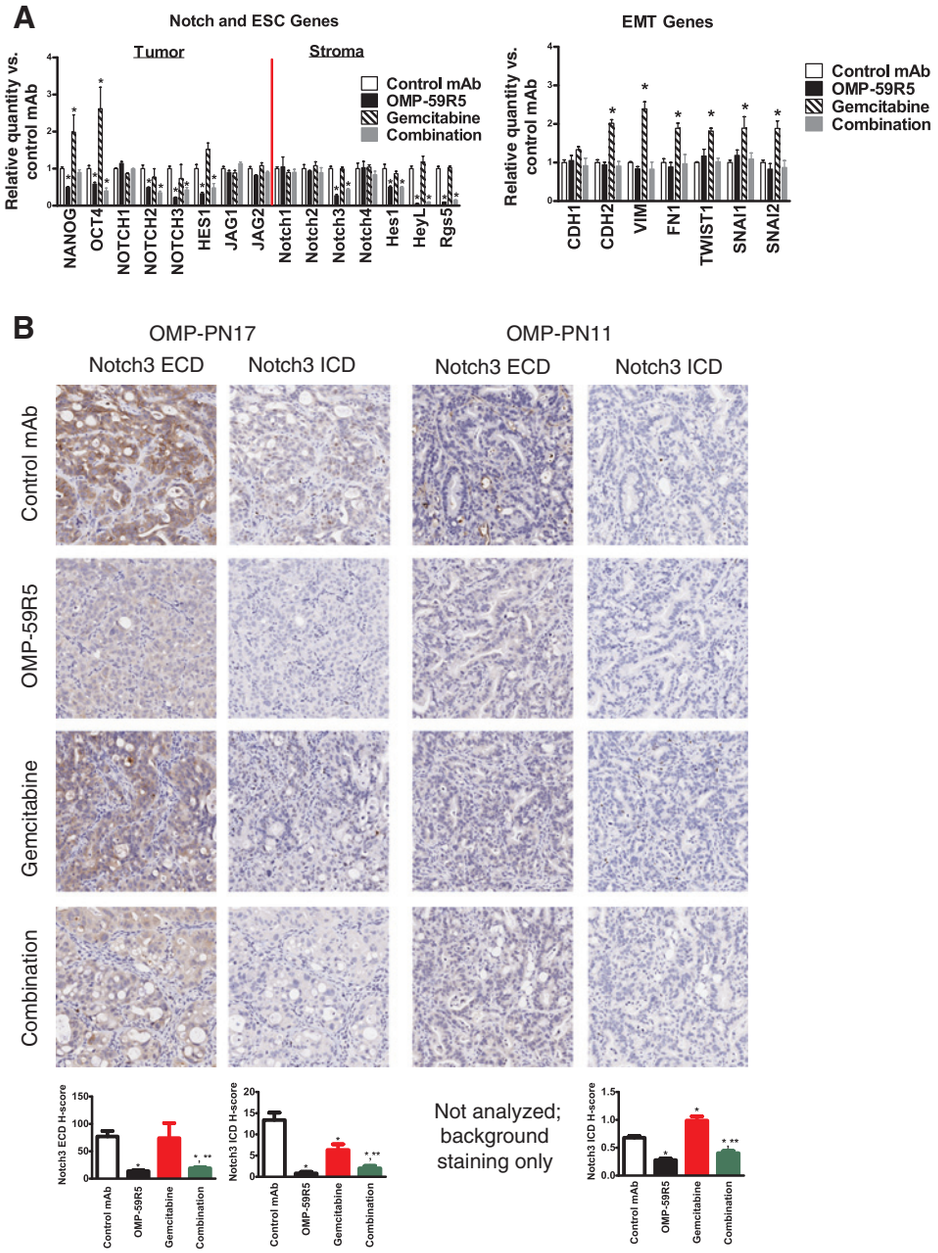

Figure 3.
Effect of OMP-59R5 on NOTCH target genes and protein expression in pancreatic xenograft tumors. A, qRT-PCR gene expression in control mAb and treated OMP-PN17 tumors at the conclusion of study (Supplementary Fig. S3). Gene expression was normalized with the housekeeping gene *GAPDH* and expressed as fold of control mAb-treated tumors. Mean ± SD, $n = 3$–4 per group. *, $P < 0.05$ versus control mAb by one-way ANOVA followed by the Tukey post-test. B, immunohistochemical analysis of Notch3 ECD and Notch3 ICD in OMP-PN17 and OMP-PN11 tumors from control and treated tumors. Magnification: ×20. Staining area and intensity were expressed as H-score. Mean ± SEM; $n = 3$–4 per group. **, $P < 0.05$ versus control mAb by the Bonferroni multiple comparison test. NA, not analyzed due to background staining only.

(Notch3 ECD) and the active form of Notch3 receptors intracellular domain (Notch3 ICD) compared with control mAb and gemcitabine in this model (Fig. 3B). In addition, tumor cells with high intensity of Notch3 ECD staining were significantly decreased by OMP-59R5 and combination treatment (>75% in both cases, $P < 0.05$). Similar results were observed by Western blot analysis in OMP-PN25 xenograft tumors (Supplementary Fig. S5C). In OMP-PN11, a tumor with low level of *NOTCH3* and did not respond to the combination therapy, Notch3 ECD was undetected, and baseline Notch3 ICD level was 10-fold lower compared with OMP-PN17. Quantitative analysis of Notch3 ICD levels in OMP-PN11 demonstrated that gemcitabine significantly increased Notch3 ICD level. Although OMP-59R5 single agent and the combination significantly reduced nuclear Notch3 ICD levels compared with control, this reduction did not influence tumor growth (Fig. 3B). It is unlikely that insensitivity to OMP-59R5 in nonresponsive tumors is due to increasing Notch1 activity upon Notch2/3 inhibition by OMP59R5 treatment as OMP-59R5 treatment decreased Notch1 ICD level in both OMP-PN11 and OMP-PN17 tumors ($P < 0.05$ in both cases), and neither gemcitabine alone nor the combination therapy modulated N1 ICD level in these tumors (Supplementary Fig. S5D). Collectively, these data suggest that Notch3 expression is regulated by a positive feedback loop and blockade of Notch2/3 signaling with OMP-59R5 impedes this autoregulatory circuit.

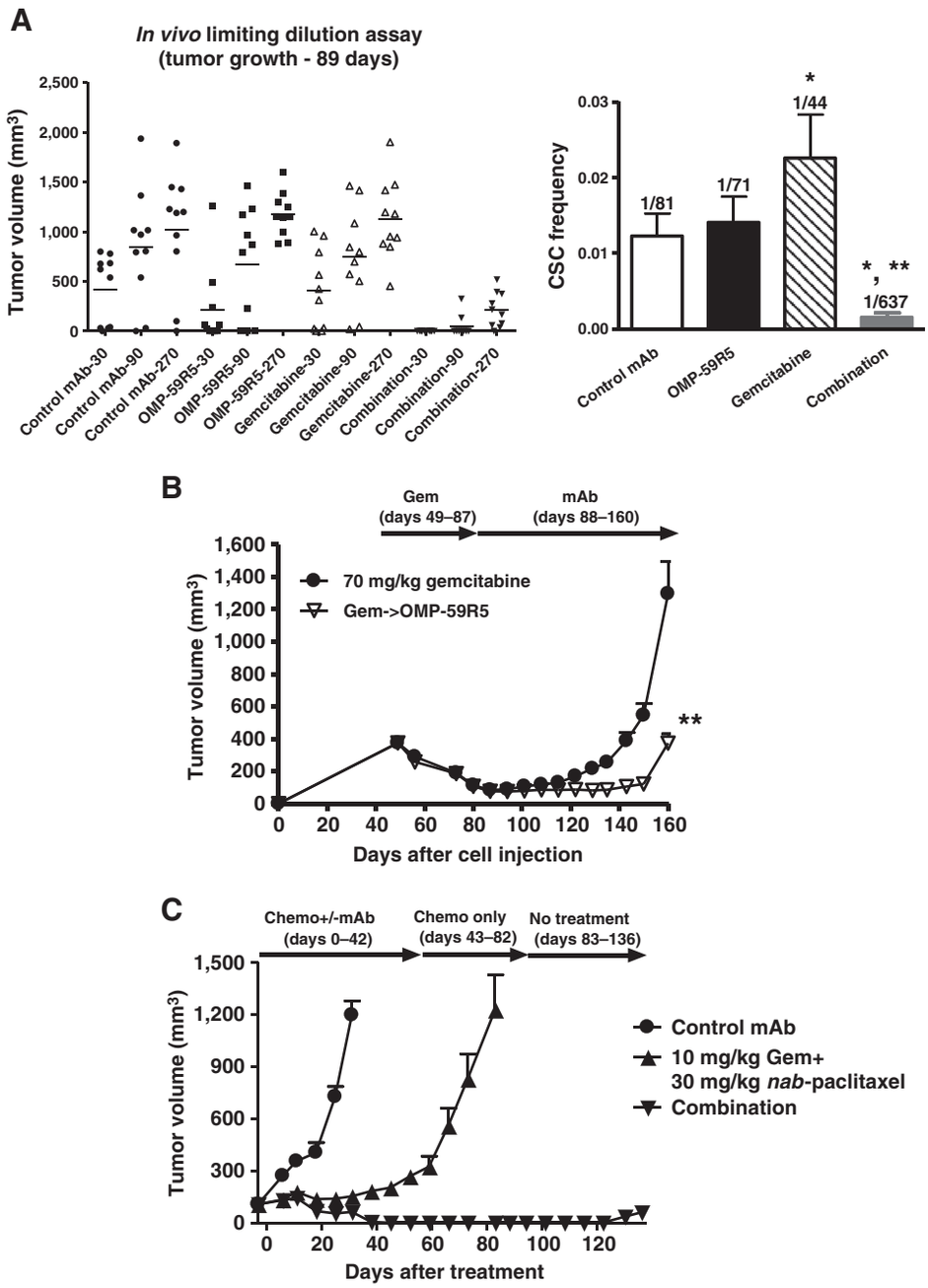

Figure 4.
Effect of OMP-59R5 on pancreatic CSC frequency and tumor recurrence after chemotherapy termination in OMP-PN8 xenograft tumors. A, LDA (left) and CSC frequency (right). Mean ± SEM; $n = 10$ animals per cell dose. *, $P < 0.05$ versus control mAb; **, $P < 0.05$ versus gemcitabine by one-way ANOVA followed by the Tukey post-test. Effect of OMP-59R5 on tumor recurrence followed by discontinuation of gemcitabine (B) and gemcitabine plus *nab*-paclitaxel (C). Mean ± SEM; $n = 9$ animals per group. **, $P < 0.05$ versus gemcitabine alone by the nonparametric *t* test.

OMP-59R5 reduces CSC frequency and delays tumor recurrence after termination of chemotherapy

To determine the functional significance of OMP-59R5 treatment on the tumorigenic potential of cells within the tumor, we carried out *in vivo* serial transplant, LDA (22) experiments (Fig. 4A, left) in OMP-PN8 xenograft tumors, a model that induced tumor regression by OMP-59R5 in combination with gemcitabine (Supplementary Fig. S3; Supplementary Table S3). This functional assay measures *in vivo* tumorigenicity and makes no assumptions about the frequency, FACS marker profile, or heterogeneity of the tumor-initiating cell population. As seen in Fig. 4A (right), control antibody-treated tumors had a CSC frequency of 1/81. Gemcitabine treatment produced a 2-fold increase in CSC frequency compared with control ($P < 0.05$). OMP-59R5 treatment alone did not alter CSC frequency compared with control (Fig. 4A) although the tumor take rate at low cell doses, that is, 30 cells and 90 cells, in the OMP-59R5 treatment group was about 50% lower than the control group. Given the fact that stem cell genes are affected by single-agent OMP-59R5 treatment indicates that the antibody has effects on stem cells in the absence of chemotherapy, and this effect may sensitize tumorigenic cells to the cytotoxic effects of chemotherapy. Indeed, the combination of OMP-59R5 and gemcitabine produced a 7-fold decrease in CSC frequency compared with control and more than 10-fold reduction in CSC

frequency compared with gemcitabine alone ($P < 0.001$ vs. gemcitabine; Fig. 4A). These results are consistent with gene expression data indicating blockade of Notch impairs the function of tumorigenic cancer stem cells.

To evaluate the effect of OMP-59R5 on tumor recurrence after chemotherapy, we treated OMP-PN8 pancreatic tumors with a high dose of gemcitabine (70 mg/kg, weekly for 5 weeks) sufficient to induce tumor regression. Four weeks after discontinuation of the gemcitabine treatment, surviving tumor cells regrew to form large tumors. On the other hand, inclusion of OMP-59R5 delayed tumor regrowth by 9 weeks after gemcitabine termination (Fig. 4B).

Recent clinical data have shown that *nab*-paclitaxel (Abraxane), an albumin-stabilized paclitaxel, is effective in combination with gemcitabine for the treatment of pancreatic ductal adenocarcinoma and has been approved by FDA as the first-line treatment of patients with metastatic adenocarcinoma of the pancreas (23). To further explore the utility of anti-Notch2/3 in the setting of pancreatic cancer, we compared antitumor efficacy of OMP-59R5 in combination with either gemcitabine or gemcitabine/*nab*-paclitaxel in OMP-PN8 xenograft tumors. When using an equivalent antitumor efficacy dose of both gemcitabine and gemcitabine/*nab*-paclitaxel, the combination of OMP-59R5 with gemcitabine/*nab*-paclitaxel induced tumor regression, whereas OMP-59R5 in combination with gemcitabine alone had less effect (Supplementary Fig. S6A). In a separate experiment, we treated OMP-PN8 xenograft tumors with either 10 mg/kg gemcitabine/30 mg/kg *nab*-paclitaxel alone or in combination with OMP-59R5 for 6 weeks. Our data demonstrate that OMP-59R5 in combination with *nab*-paclitaxel and gemcitabine resulted in striking tumor regression in 10 of 10 mice, whereas tumors treated with chemotherapeutic agents alone grew continuously (Fig. 4C). The effect of the triple combination of anti-Notch2/3, gemcitabine, and *nab*-paclitaxel was quite durable and persisted after both antibody and chemotherapeutic treatments were discontinued. Similar observations were seen in OMP-PN16 xenograft tumors where the triple combination of OMP-59R5 with gemcitabine/*nab*-paclitaxel resulted in tumor regression (Supplementary Fig. S6C).

Antitumor activity of OMP-59R5 in breast, ovarian, and small-cell lung cancer

In addition to pancreatic tumors, we also observed antitumor efficacy by anti-Notch2/3 antibody in breast, ovarian, and small-cell lung xenograft tumors. OMP-59R5 was efficacious as a single agent in UM-PE13 (a triple-negative breast tumor), OMP-OV38 (a serous ovarian tumor), and OMP-LU40 (a small-cell lung cancer; Fig. 5A and B and Supplementary Fig. S7A) and combination activity with the chemotherapeutic agent in UM-PE13, OMP-OV38, and OMP-LU68 (Fig. 5A and B and Supplementary Fig. S7A). qRT-PCR gene expression analysis in UM-PE13 and OMP-OV38 tumors showed that *HES1*, *NOTCH2*, and *NOTCH3* in the tumors and *Notch3*, *Hes1*, *HeyL*, and *Rgs5* in the stroma were robustly downregulated by OMP-59R5 in these models (Fig. 5C and D). Immunohistochemistry analysis in UM-PE13 revealed that the antitumor activity of OMP-59R5 was associated with a 4-fold decrease in Notch3 ICD (Supplementary Fig. S7B). When high doses of chemotherapy induced tumor regression in UM-PE13 and OMP-LU68 tumors, the combination of OMP-59R5 with the chemotherapeutic agents delayed tumor recurrence following discontinuation of the chemotherapeutic agents compared with the rate of tumor recurrence after treatment with the chemotherapeutic agents alone (Fig. 5E and F). In the UM-PE13 breast tumor, OMP-59R5 treatment decreased CSC frequency to 37% relative to the control, whereas the residual tumor cells after paclitaxel treatment were enriched in CSCs exhibiting an approximately 2-fold increase in CSC frequency compared with the control (Fig. 5H). Importantly, the combination of anti-Notch2/3 and paclitaxel treatment decreased CSC frequency and tumorigenicity in the residual tumor cells, resulting in a 10-fold reduction in CSC frequency compared with the paclitaxel only-treated group. Similar observations were found in OMP-LU40 xenograft tumors (Fig. 5G). Taken together, these findings indicate the cross-reactive Notch2/3 targeting antibody OMP-59R5 is efficacious in a wide range of solid tumors, inhibiting Notch signaling in both tumor and stromal cells while reducing tumorigenic cell frequency.

OMP-59R5 alters pericyte coverage in tumor vasculature

In our experiments, we observed that *Rgs*5, a marker of developing pericytes, was consistently downregulated by OMP-59R5 in various tumors. Pericytes are tightly associated with endothelial cells in normal vasculature to provide structural support to blood vessels and regulate tissue physiology by modulating vascular stability, whereas pericytes in tumor vasculature exhibit abnormal shapes and are loosely associated with endothelial cells on tumor capillaries (24). Hamzah and colleagues reported that reduction of *Rgs*5 expression in an endocrine pancreatic tumor model results in pericyte maturation, "normalizes" tumor vasculature, and improves the delivery of chemotherapeutic agents and the immune response against the tumor (25). Similarly, patients with breast cancer with mature pericyte coverage demonstrate improved disease-free survival and overall survival (26). To investigate the functional significance of OMP-59R5–mediated downregulation of *Rgs*5 and its effect on pericytes, we conducted immunofluorescence staining for desmin, a marker of mature pericytes (24). We found that desmin-positive pericytes in the vasculature were closely associated with vessels in tumors treated with OMP-59R5, suggesting pericyte recruitment to endothelial cells and subsequent vascular maturation (Fig. 6A). To determine whether mature pericytes are linked to a functional vasculature, we visualized plant lectin (tomato)-perfused vessels pretreated with pimonidazole. As seen in Supplementary Fig. S8A, pericytes either overlap or are more closely associated with the endothelial cells in perfused vessels. OMP-59R5 and gemcitabine treatment increased perfused blood vessels per area by 15%. An additional 20% increase in perfused vessels was seen in tumors after treatment with the combination of anti-Notch2/3 and gemcitabine (Fig. 6B and Supplementary Fig. S8B). The increase in perfusion in treated tumors was associated with a reduced tumor hypoxia (Fig. 6C), more evident in tumors treated with the combination of OMP-59R5 and gemcitabine compared with control mAb-treated tumors. These findings suggest an improved oxygen supply in the tumors as a result of improved pericyte coverage and vascular normalization by OMP-59R5 treatment.

Discussion

Notch signaling plays an important role in regulating cell fate decisions in a variety of normal tissues (1). Several lines of evidence have indicated that dysregulation of the Notch pathway can lead to uncontrolled self-renewal of CSCs which generate

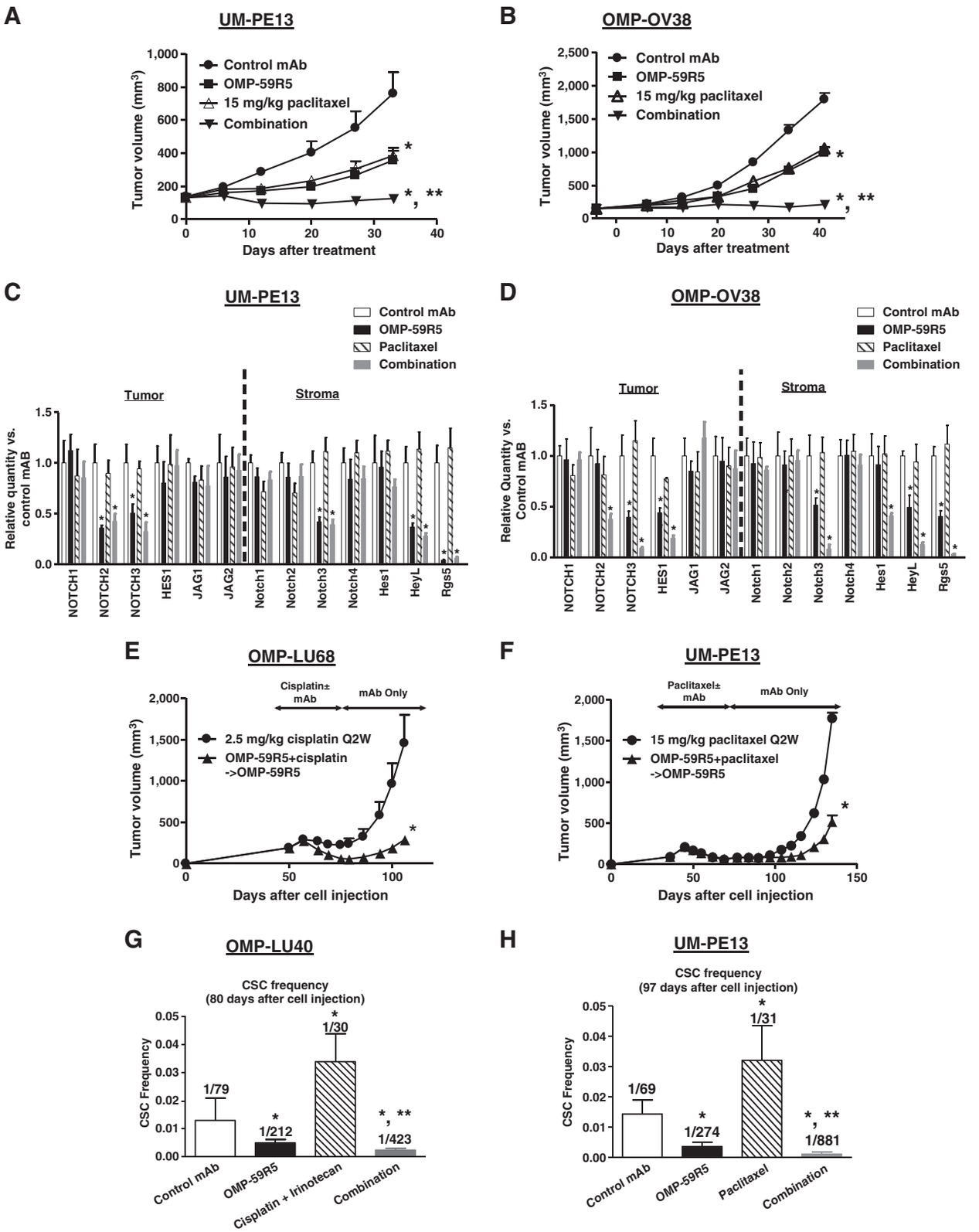

Figure 5.
Activity of OMP-59R5 on breast, ovarian, and small-cell lung xenograft tumors. A and B, antitumor effect of OMP-59R5 in UM-PE13 (triple-negative breast tumor) and OMP-OV38 (serous ovarian tumor). Mean ± SEM; $n = 8$–10 animals per group. *, $P < 0.05$ versus control mAb; **, $P < 0.05$ versus single agents by two-way ANOVA followed by the Bonferroni post-test comparison. (*Continued on the following page.*)

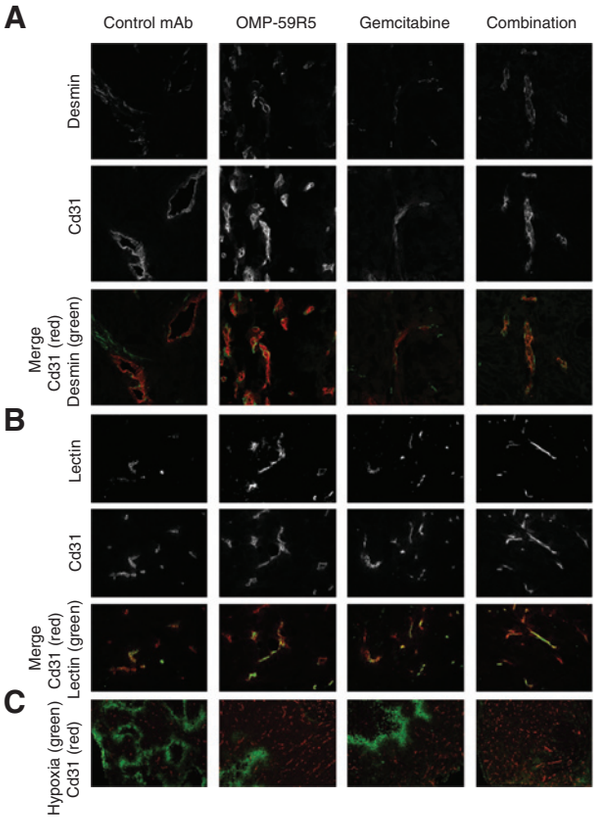

Figure 6.
Effect OMP-59R5 on mature pericytes, vascular perfusion, and tumor hypoxia. A, histologic analysis of mature pericyte marker desmin (green), endothelial cell marker Cd31 (red), in OMP-PN17 xenograft tumors. Colocalization of both markers is shown in yellow. B, detection of perfused vasculature. Tomato Lectin was administered by intravenous injection 5 minutes before tumor removal. C, antipimonidazole-labeled hypoxic tumor cells (green) with Cd31 (red). $N = 3$–4 tumors per group. Magnifications: ×60 (A), ×20 (B), and ×4 (C).

tumors that are resistant to conventional therapies (27). We sought to determine whether interference with CSC self-renewal ability through blocking Notch2/3 signaling would overcome treatment resistance. Using PDX models, we demonstrate that chemotherapeutic agents were largely ineffective in reducing CSC frequency, whereas blockade of Notch2/3 signaling by OMP-59R5 reduced CSC frequency in combination with chemotherapeutic agents in various cancer models examined. We further demonstrate that the triple combination of anti-Notch2/3 with gemcitabine plus *nab*-paclitaxel (Abraxane, a protein-bound paclitaxel) chemotherapy doublet, a new standard-of-care regimen for treatment of pancreatic cancer (23), produced striking tumor regression in pancreatic cancer xenografts, suggesting that this may be a beneficial approach for the treatment of pancreatic cancer. The ongoing ALPINE clinical trial combining OMP-59R5 (tarextumab) with gemicitabine and *nab*-paclitaxel is designed to test this possibility (clinicaltrials.gov).

In this study, we observed a strong positive correlation between baseline *NOTCH3* gene expression and the antitumor activity of OMP-59R5 plus gemcitabine in pancreatic tumors. The sensitivity of these tumors to the combination therapy is independent of Kras mutation status, gemcitabine sensitivity, or molecular subtype of pancreatic ductal adenocarcinoma. These data indicate that Notch3 expression may be a useful predictive marker to identify patients most likely to respond to OMP-59R5. In *NOTCH3* high tumors, OMP-59R5 treatment induced a significant decrease in both Notch3 ECD and Notch3 ICD protein levels, suggesting that *NOTCH3* gene expression is an important determinant of Notch3 signaling-mediated growth of these tumors. Indeed, Notch3 expression has been associated with disease stage, poorer overall survival, and resistance to chemotherapy in solid tumors (5, 7, 9). The low sensitivity to OMP-59R5 in nonresponsive tumors is not likely due to loss-of-function mutations in ligand-binding domain/other functional regions of NOTCH2/3 or due to OMP-59R5–induced Notch1 activation in nonresponsive tumors, as whole-exome sequencing of our PDX tumors showed no mutations in either *NOTCH2* or *NOTCH3* that result in amino acid substitutions in EGF repeats involved in ligand binding, and Notch1 ICD level was not increased by the combination therapy in either responsive and nonresponsive tumors. Although no correlation between baseline *NOTCH2* gene expression and tumor response to the combination therapy was observed, *NOTCH2* gene was downregulated by OMP-59R5 treatment alone and by the combination therapy, suggesting that Notch2 signaling in the tumors and/or stroma niche may cooperate with Notch3 signaling to facilitate tumor growth.

We observed that EMT and stem cell gene sets were upregulated in tumors by gemcitabine. Combination with anti-Notch2/3 treatment reversed the increase in gemcitabine-induced EMT gene sets and downregulated stem cell gene sets. Real-time PCR gene expression and immunohistochemical analyses in OMP-59R5 responsive pancreatic xenograft tumors further confirmed microarray findings. Our data are consistent with literature reports suggesting that acquisition of EMT contributes to drug resistance and that EMT plays an important role in the generation of CSCs (28).

In the current study, we observed striking downregulation of *Rgs5* in the stroma by OMP-59R5 treatment in various tumors. *Rgs5* and *Notch3* are coexpressed in pericytes and are known to play an essential role in regulating the functions of these cells (29). Previous studies have suggested that simultaneous inhibition of endothelial cells and pericytes results in an additive effect of disrupting tumor angiogenesis and thereby reducing tumor growth (30). Other studies have shown that loss of *Rgs5* gene expression modulates tumor angiogenesis by inducing pericyte maturation, vascular normalization, and reducing tumor hypoxia and vessel leakiness (25). Our data demonstrate that OMP-59R5

(*Continued.*) C and D, qRT-PCR gene expression in the tumor and stroma in UM-PE13 and OMP-OV38 xenograft tumors at the end of study from A and B. Gene expression was normalized with the housekeeping gene *GAPDH* and expressed as fold of control mAb-treated tumors. Mean ± SD; $n = 3$–4 per group. *, $P < 0.05$ versus control mAb by one-way ANOVA followed by the Tukey post-test. E and F, effect of OMP-59R5 on tumor recurrence in OMP-LU68 (small-cell lung tumors) and UM-PE13. Mean ± SEM; $n = 10$ animals per group. *, $P < 0.05$ versus chemotherapeutic agent alone by the nonparametric *t* test. G and H, effect of OMP-59R5 on CSC frequency in OMP-LU40 (small-cell lung tumor) and UM-PE13 tumors at the end of study from Supplementary Fig. S6A (OMP-LU40) and F (UM-PE13). Mean ± SEM; $n = 10$ animals per group. *, $P < 0.05$ versus control mAb; **, $P < 0.05$ versus gemcitabine by one-way ANOVA followed by the Tukey post-test.

treatment decreases *Rgs5* gene expression, modulates intratumoral pericyte localization, and increases vessel perfusion while reducing tumor hypoxia. OMP-59R5–mediated improvement in vasculature functions may increase drug delivery to the tumors, thereby enhancing the antitumor efficacy, particularly in combination with chemotherapeutic agents or other treatment modalities. In contrast to anti-Notch2/3, inhibition of DLL4/Notch signaling using DLL4-specific inhibitors has been shown to induce dense vasculature network of unperfused and poorly differentiated vessels (31, 32). Consistent with these previous studies, in an small-cell lung cancer xenograft model, we found that tumors treated with an anti-mouse DLL4 antibody resulted in an increased intratumoral hypoxia and hyperproliferation of the endothelial cells, whereas blocking Notch2/3 signaling by OMP-59R5 produced an opposite effect on tumor vasculatures/stroma versus targeting DLL4/Notch signaling by anti-mouse DLL4 antibody (Supplementary Fig. S8C). "Normalization" of tumor vasculature was reported previously in both preclinical tumor models and in patients with cancer receiving anti-VEGF therapy (reviewed in ref. 33).

In summary, our findings provide evidence for the utility of targeting Notch2 and Notch3 for cancer treatment. Our data also suggest that therapeutic approaches targeting pathways important for CSCs may improve treatment outcome and overall survival. Our recent phase I data indicate that tarextumab is generally well tolerated and show signs of antitumor efficacy and modulation of Notch pathway signaling in the clinic (34). On the basis of the preclinical studies described here, we are evaluating the utility of Notch3 gene expression as a predictive biomarker in our ongoing clinical studies and also the testing the ability of tarextumab to modulate Notch and CSC gene signatures.

Disclosure of Potential Conflicts of Interest

No potential conflicts of interest were disclosed.

Authors' Contributions

Conception and design: W.-C. Yen, J. Cain, A. Sato, A.M. Kapoun, J. Lewicki, A. Gurney, T. Hoey

Development of methodology: M. Fischer, J. Lewicki

Acquisition of data (provided animals, acquired and managed patients, provided facilities, etc.): W.-C. Yen, M. Fischer, F. Axelrod, C. Bond, J. Cain, B. Cancilla, J. Shah, T. Tang, B. Wallace, A.M. Kapoun

Analysis and interpretation of data (e.g., statistical analysis, biostatistics, computational analysis): W.-C. Yen, M. Fischer, F. Axelrod, J. Cain, R. Henner, R. Meisner, J. Shah, T. Tang, B. Wallace, M. Wang, C. Zhang, A.M. Kapoun, T. Hoey

Writing, review, and/or revision of the manuscript: W.-C. Yen, M. Fischer, J. Cain, T. Tang, M. Wang, J. Lewicki, A. Gurney, T. Hoey

Administrative, technical, or material support (i.e., reporting or organizing data, constructing databases): M. Fischer

Study supervision: J. Lewicki, T. Hoey

Acknowledgments

The authors thank Inkyung Park, Jim Evans, Raymond Tam, Akbar Currimbhoy, Fiore Cattaruzza, Pete Yeung, Kellie Pickell, Xiaomei Song, and many people at OncoMed Pharmaceuticals, Inc., for their contributions to this work.

The costs of publication of this article were defrayed in part by the payment of page charges. This article must therefore be hereby marked *advertisement* in accordance with 18 U.S.C. Section 1734 solely to indicate this fact.

Received November 1, 2014; revised January 13, 2015; accepted January 14, 2015; published online May 1, 2015.

References

1. Penton AL, Leonard LD, Spinner NB. Notch signaling in human development and disease. Semin Cell Dev Biol 2012;23:450–7.
2. Lin L, Mernaugh R, Yi F, Blum D, Carbone DP, Dang TP. Targeting specific regions of the Notch3 ligand-binding domain induces apoptosis and inhibits tumor growth in lung cancer. Cancer Res 2010;70:632–8.
3. Park JT, Li M, Nakayama K, Mao TL, Davidson B, Zhang Z, et al. Notch3 gene amplification in ovarian cancer. Cancer Res 2006;66:6312–8.
4. Yamaguchi N, Oyama T, Ito E, Satoh H, Azma S, Hayashi M, et al. NOTCH3 signaling pathway plays crucial roles in the proliferation of ErbB2-negative human breast cancer cells. Cancer Res 2008;68:1881–8.
5. Doucas H, Mann CD, Sutton CD, Garcea G, Neal CP, Berry DP, et al. Expression of nuclear Notch3 in pancreatic adenocarcinomas is associated with adverse clinical features, and correlates with the expression of STAT3 and phosphorylated Akt. J Surg Oncol 2008;97:63–8.
6. Mazur PK, Einwachter H, Lee M, Sipos B, Nakhai H, Rad R, et al. Notch2 is required for progression of pancreatic intraepithelial neoplasia and development of pancreatic ductal adenocarcinoma. Proc Natl Acad Sci U S A 2010;107:13438–43.
7. Ozawa T, Kazama S, Akiyoshi T, Murono K, Yoneyama S, Tanaka J, et al. Nuclear Notch3 expression is associated with tumor recurrence in patients with stage II and III colorectal cancer. Ann Surg Oncol 2014;21:2650–8.
8. Sainson RC, Harris AL. Regulation of angiogenesis by homotypic and heterotypic notch signalling in endothelial cells and pericytes: from basic research to potential therapies. Angiogenesis 2008;11:41–51.
9. Nguyen LV, Vanner R, Dirks P, Eaves CJ. Cancer stem cells: an evolving concept. Nat Rev 2012;12:133–43.
10. Malik B, Nie D. Cancer stem cells and resistance to chemo and radio therapy. Front Biosci 2012;4:2142–9.
11. Takebe N, Nguyen D, Yang SX. Targeting Notch pathway in cancer: clinical development advances and challenges. Pharmacol Ther 2014;141:140–9.
12. Rothe C, Urlinger S, Lonhning C, Prassler J, Stark Y, Jagur U, et al. The human combinatorial library HuCAL GOLD combines diversification of all six CDRs according to the natural immune system with a novel display method for efficient selection of high-affinity antibodies. J Mol Biol 2008; 376:1182–200.
13. Hoey T, Yen WC, Axelrod F, Basi J, Donigian L, Dylla S, et al. DLL4 blockade inhibits tumor growth and reduces tumor-initiating cell frequency. Cell Stem Cell 2009;5:168–77.
14. Dalerba P, Guiducci C, Poliani PL, Cifola I, Parenza M, Frattini M, et al. Phenotypic characterization of human colorectal cancer stem cells. Proc Natl Acad Sci U S A 2007;104:10158–63.
15. Baldi P, Long AD. A Bayesian framework for the analysis of microarray expression data: regularized t-test and statistical inferences of gene changes. Bioinformatics 2011;17:509–19.
16. Garrido-Laguna I, Uson M, Rajeshkumar NV, Tan AC, de Oiveira E, Karikari C, et al. Tumor engraftment in nude mice and enrichment in stroma-related gene pathways predict poor survival and resistance to gemitabine in patients with pancreatic cancer. Clin Cancer Res 2011; 17:5793–800.
17. Hidalgo M, Bruckheimer E, Rajeshkumar NV, Garrido-Laguna I, de Oiveira E, Rubio-Viqueira B, et al. A pilot clinical study of treatment guided by personalized tumorgrafts in patients with advanced cancer. Mol Cancer Ther 2011;10:1311–6.
18. Collisson EA, Sadanandam A, Olson P, Gibb WJ, Truitt M, Gu S, et al. Subtypes of pancreatic ductal adenocarcinoma and their differing responses to therapy. Nat Med 2011;17:500–4.
19. Yen WC, Fischer MM, Hynes M, Wu J, Kim E, Beviglia L, et al. Anti-DLL4 has broad spectrum activity in pancreatic cancer dependent on targeting DLL4-Notch signaling in both tumor and vasculature cells. Clin Cancer Res 2012; 18:5374–86.

20. Ben-Porath I, Thomson MW, Carey VJ, Ge R, Bell GW, Regev A, et al. An embryonic stem cell-like signature in poorly differentiated aggressive human tumors. Nat Genet 2008;40:499–507.
21. Bergers G, Song S. The role of pericytes in blood-vessel formation and maintenance. Neuro Oncol 2005;7:452–64.
22. Wang JC, Doedens M, Dick JE. Primitive human hematopoietic cells are enriched in cord blood compared with adult bone marrow or mobilized peripheral blood as measured by the quantitative in vivo SCID-repopulating cell assay. Blood 1997;89:3919–24.
23. Von Hoff DD, Ervin T, Arena FP, Chiorean EG, Infante J, Moore M, et al. Increased survival in pancreatic cancer with nab-paclitaxel plus gemcitabine. N Engl J Med 2013;369:1691–703.
24. Barlow K, Sahders AM, Soker S, Ergun S, Metheny-Barlow LJ. Pericytes on the tumor vasculature: Jekyll or Hyde? Cancer microenvironment 2013; 6:1–17.
25. Hamzah J, Jugold M, Kiessling F, Rigby P, Manzur M, Marti HH, et al. Vascular normalization in Rgs5-deficient tumours promotes immune destruction. Nature 2008;453:410–4.
26. Cooke VG, LeBleu VS, Keskin D, Khan Z, O'Connell JT, Teng Y, et al. Pericyte depletion results in hypoxia-associated epithelial-to-mesenchymal transition and metastasis mediated by met signaling pathway. Cancer Cell 2012;21:66–81.
27. Wang J, Sullenger BA, Rich JN. Notch signaling in cancer stem cells. Expt Med Biol 2012;727:174–85.
28. Scheel C, Weinberg RA. Cancer stem cells and epithelial-mesenchymal transition: concepts and molecular links. Semin Cancer Biol 2012;22: 396–403.
29. Lovschall H, Mitsiadis TA, Poulsen K, Jensen KH, Kjeldsen AL. Coexpression of Notch3 and Rgs5 in the pericyte-vascular smooth muscle cell axis in response to pulp injury. Int J Dev Biol 2007;51: 715–21.
30. Kuhnert F, Tam BY, Sennino B, Gray JT, Yuan J, Jocson A, et al. Soluble receptor-mediated selective inhibition of VEGFR and PDGFRbeta signaling during physiologic and tumor angiogenesis. Proc Natl Acad Sci U S A 2008;105:10185–90.
31. Noguera-Troise I, Daly C, Papadopoulos NJ, Coetzee S, Boland P, Gale NW, et al. Blockade of DLL4 inhibits tumor growth by promoting non-productive angiogenesis. Nature 2006;444:1032–7.
32. Ridgway J, Zhang G, Wu Y, Stawicki S, Liang WC, Chanthery Y, et al. Inhibition of DLL4 signaling inhibits tumor growth by deregulating angiogenesis. Nature 2006;444:1083–7.
33. Goel S, Duda DG, Xu L, Munn LL, Boucher Y, Fukumura D, et al. Normalization of the vasculature for treatment of cancer and other diseases. Physiol Rev 2011;91:1071–121.
34. Smith DC, Chugh R, Patnaik A, Papadopoulos K, Chambers G, Thorpe V, et al. A first-in-human phase 1 study to evaluate the fully human monoclonal antibody OMP-59R5 (anti-Notch2/3) administered intravenously to patients with advanced solid tumors. Eur J Cancer 2012;48 Suppl 6:11–2.